

Redox Control and High Conductivity of Nickel Bis(dithiolene) Complex π -Nanosheet: A Potential Organic Two-Dimensional Topological Insulator

Tetsuya Kambe,[†] Ryota Sakamoto,[†] Tetsuro Kusamoto,[†] Tigmansu Pal,[†] Naoya Fukui,[‡] Ken Hoshiko,[†] Takahiro Shimojima,[§] Zhengfei Wang,^{||} Toru Hirahara,^{‡,⊥} Kyoko Ishizaka,[§] Shuji Hasegawa,[‡] Feng Liu,^{||} and Hiroshi Nishihara^{*,†}

[†]Department of Chemistry, Graduate School of Science, The University of Tokyo, 7-3-1, Hongo, Bunkyo-ku, Tokyo 113-0033, Japan

[‡]Department of Physics, Graduate School of Science, The University of Tokyo, 7-3-1, Hongo, Bunkyo-ku, Tokyo 113-0033, Japan

[§]Quantum-Phase Electronics Center (QPEC) and Department of Applied Physics, Graduate School of Engineering, The University of Tokyo, 7-3-1, Hongo, Bunkyo-ku, Tokyo 113-8656, Japan

^{||}Department of Materials Science and Engineering, University of Utah, Salt Lake City, Utah 84112, United States

S Supporting Information

ABSTRACT: A bulk material comprising stacked nanosheets of nickel bis(dithiolene) complexes is investigated. The average oxidation number is $-3/4$ for each complex unit in the as-prepared sample; oxidation or reduction respectively can change this to 0 or -1 . Refined electrical conductivity measurement, involving a single microflake sample being subjected to the van der Pauw method under scanning electron microscopy control, reveals a conductivity of $1.6 \times 10^2 \text{ S cm}^{-1}$, which is remarkably high for a coordination polymeric material. Conductivity is also noted to modulate with the change of oxidation state. Theoretical calculation and photoelectron emission spectroscopy reveal the stacked nanosheets to have a metallic nature. This work provides a foothold for the development of the first organic-based two-dimensional topological insulator, which will require the precise control of the oxidation state in the single-layer nickel bisdithiolene complex nanosheet (cf. Liu, F. et al. *Nano Lett.* **2013**, *13*, 2842).

Increasing attention has been paid to nanosheets (two-dimensional crystalline materials), such as graphene^{1–5} and MoS₂.^{6–9} These nanosheets are promising for use in innovative electronic^{10,11} and optonic^{12–14} devices. A nickel bis(dithiolene) complex nanosheet created by the authors is part of a new class of two-dimensional material (Figure 1a).^{15,16} It is distinctive for its bottom-up synthesis from molecular and ionic components (benzenhexathiol and nickel(II) ions) that results in a single-layer nanosheet. It also features a hexagonal kagomé lattice comprising phenylene linkers and nickel bis(dithiolene) complex units in a π -conjugated electronic structure. It is thus the first conductive bottom-up nanosheet.

The topological insulator (TI) is a new state of matter.^{17–20} Its bulk part is an insulator, but its edges (i.e., surfaces or sides) feature a metallic phase. The metallic edge is spin-polarized and, thereby, conveys a spin current. These features make TIs promising materials for electronics and spintronics. TIs

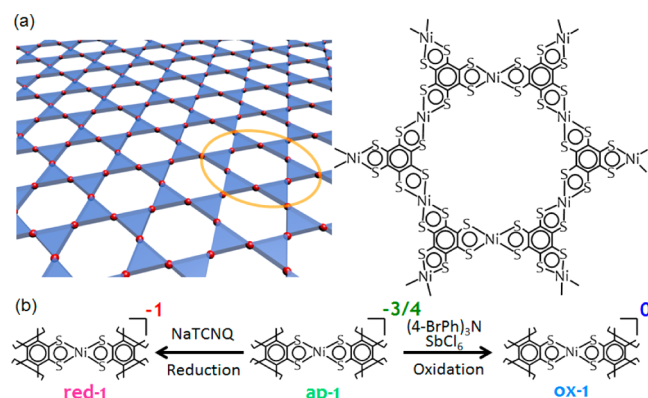


Figure 1. (a) Illustration of the chemical structure of the nickel bis(dithiolene) complex nanosheet. **1** corresponds to the stacked nanosheet. (b) Schematic illustration on redox control in **1**.

reported thus far are all inorganic materials. Bi₂Se₃^{21–29} is a representative three-dimensional TI; two-dimensional TIs (2D-TIs) are rarer, with the only known examples being a quantum well composed of HgTe/CdTe^{31,32} and a Bi bilayer on Bi₂Te₃.^{33,34} Besides, organic-based TI systems remain unexplored.

The authors predicted a two-dimensional network of Ph₃M (M = Pb or Bi) as a potential organic 2D-TI,³⁵ but it is hardly accessible. The authors also suggested a realizable candidate, the single-layer nickel bis(dithiolene) complex nanosheet (Figure 1a).³⁶ For this nanosheet to function as a 2D-TI, it requires precise control of its doping, so that the Fermi level locates in the gapped Dirac point. Herein, control in the oxidation state of the nickel bis(dithiolene) complex unit is equivalent to a modulation of the doping level: For example, an average oxidation number of $-2/3$ is suitable for a 2D-TI.³⁶

The present report concentrates on two topics: the control of the oxidation state of the nickel bis(dithiolene) complex

Received: August 1, 2014

Published: September 24, 2014

nanosheet (Figure 1b), which is important in making a 2D-TI, and the use of a sophisticated conductivity measurement method. Measurements are made employing the van der Pauw method using a four-probe set-up under the inspection of scanning electron microscopy (SEM), which gives a genuine electrical conductivity excluding a contact resistance. Associated with the conductivity measurement, photoelectron spectroscopy (PES) and first-principles calculations are conducted to investigate the band structure. Handling and size limitations lead to samples of stacked nanosheets (hereafter called **1**) being used in this series of studies.

To control the oxidation state, as-prepared **1** (**ap-1**) was oxidized using tris(4-bromophenyl)aminium hexachloroantimonate and reduced using NaTCNQ to give samples respectively labeled **ox-1** and **red-1**. The oxidation state was then investigated by X-ray photoelectron spectroscopy (XPS), where its S 2s peak sharply reflects the oxidation state of the bis(dithiolene) metal complex (Figure 2).³⁷ **Ap-1** showed an

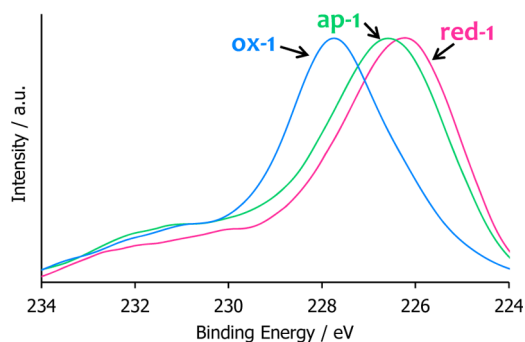


Figure 2. S 2s peak for the XPS of **1** (blue: **ox-1**; green: **ap-1**; red: **red-1**).

average oxidation number of $-3/4$ for the nickel bis(dithiolene) unit.¹⁵ The S 2s envelope could be deconvoluted into three peaks, corresponding to the shake-up peak often found in the dithiolene-type compound,^{38,39} the -1 oxidation state for the nickel bis(dithiolene) unit, and the zero oxidation state, respectively (Figure S1). The S 2s envelope shifted toward higher binding energies upon oxidation, whereas reduction decreased the binding energy. The deconvolution of the S 2s peak suggests that the nickel bis(dithiolene) complex unit was monovalent, being in the 0 and -1 states in **ox-1** and **red-1**, respectively (Figures S2 and S3). These results suggest that an electrochemical doping channel is available in the nickel bis(dithiolene) complex nanosheet.

Our previous work had reported the electrical conductivity of pelletized samples of **1** measured using a primitive two-electrode set-up.¹⁵ Here we employed an upgraded measurement technique. Each single microflake of **ox-1** and **ap-1** was subjected to the van der Pauw method under the control of SEM⁴⁰ (Figures 3a,b, S4, and S5). This measurement excluded resistances derived from the contact between the probe and the sample and also the grain boundary of the sample, thereby giving the intrinsic conductivity. **Ox-1** showed an electrical conductivity of $1.6 \times 10^2 \text{ S cm}^{-1}$ at 300 K, which is, to the best of our knowledge, the highest value for coordination polymers.^{41–45} A two-dimensional Cu(I) 4-hydroxythiophenolate network features an electrical conductivity of $1.2 \times 10^2 \text{ S cm}^{-1}$,⁴¹ whereas a recently reported metal–organic framework or porous coordination polymer (MOF or PCP) comprising the nickel bis(diimine) complex motif (with the

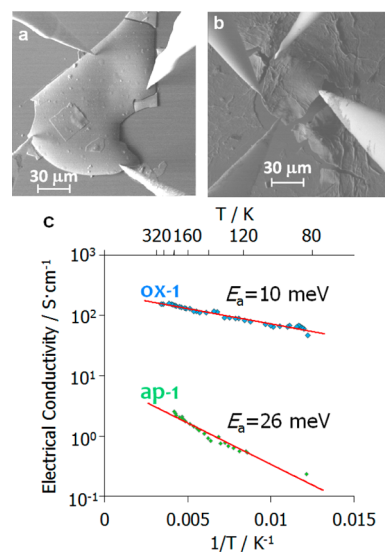


Figure 3. (a,b) SEM images for the van der Pauw measurement of **ox-1** and **ap-1**, respectively. (c) Temperature dependence of the electrical conductivity for **ox-1** and **ap-1**. Sample thickness: $1 \mu\text{m}$. The conductivity contains an error of 10%.

same electronic structure as the bis(dithiolene) complex motif) has been reported to possess a conductivity of $4.0 \times 10 \text{ S cm}^{-1}$ at room temperature.⁴⁵ **Ap-1**, however, showed a conductivity that was smaller by 2 orders of magnitude (2.8 S cm^{-1} at 300 K). Figure 3c shows the temperature dependence of the conductivity, which decreased slightly with falling temperature. The linear relationship between the logarithm of the temperature with respect to the reciprocal of the temperature in the Arrhenius plot gives the activation energy (E_a) of each sample (**ox-1**: 10 meV; **ap-1**: 26 meV). The E_a of **ox-1** appears quite small for a coordination polymer.

To reveal the origin of the observed high electrical conductivity and small activation energy, **ap-1** was subjected to PES. **Ap-1** on highly oriented pyrolytic graphite (HOPG) exhibited a Fermi edge even at 300 K: The Fermi edge was more prominent at 17 K (Figure 4). This result suggests a metallic nature. The band structure of **1** is also reproduced in first-principles calculation (Figure 5). The structure is based on

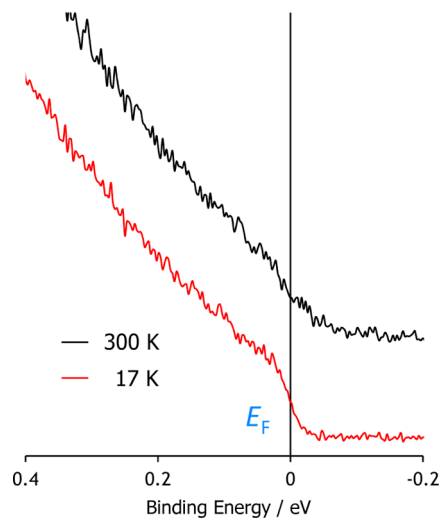


Figure 4. PES of **ap-1** acquired at 300 and 17 K.

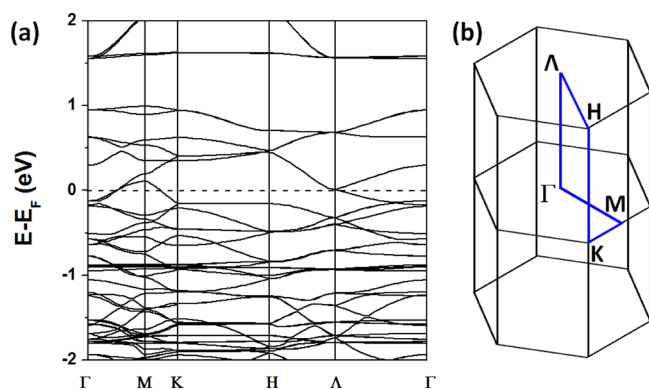


Figure 5. (a) First-principles band structure of **ox-1**. (b) Corresponding first Brillouin zone and high-symmetry k-points.

that suggested by powder X-ray diffraction analysis,¹⁵ and the oxidation number of the nickel bis(dithiolene) unit considered herein is zero (i.e., **ox-1**). The band structure also indicates a metallic nature (Figure 5).

Both PES and the band calculation suggest that **ox-1** and **ap-1** are metallic, although the van der Pauw conductivity measurement revealed semiconductive behavior with small E_a . This discrepancy might stem from a structural disorder in the sample. Particularly, **ap-1** contained Na^+ as a counterion, which could have amplified the structural confusion.

In conclusion, the oxidation state of **1** was controlled via chemical oxidation and reduction, which fixed the valence of the nickel bis(dithiolene) complex unit at 0 and -1 , respectively. The electrical conductivity of a single microflake of **1** was evaluated using the van der Pauw method under the control of SEM; it showed a very high conductivity of $1.6 \times 10^2 \text{ S cm}^{-1}$ at 300 K. The metallic nature of **1** was confirmed by PES and first-principles calculations. This work establishes a remarkable area of progress in coordination polymer chemistry and will be a sound step toward the realization of an organic 2D-TI.

■ ASSOCIATED CONTENT

Supporting Information

Experimental details, deconvolution of the S 2s peaks in XPS, close-ups of typical SEM images for **ox-1** and **ap-1** showing flat and smooth textures, and typical $V-I$ plots for **ox-1** and **ap-1** in the van der Pauw measurement. This material is available free of charge via the Internet at <http://pubs.acs.org>.

■ AUTHOR INFORMATION

Corresponding Author

nishihara@chem.s.u-tokyo.ac.jp

Present Address

[†]Department of Condensed Matter Physics, Graduate School of Science and Engineering, Tokyo Institute of Technology, 2-12-1, Ookayama, Meguro-ku, Tokyo 152-8551, Japan.

Notes

The authors declare no competing financial interest.

■ ACKNOWLEDGMENTS

This work was supported by Grants-in-Aid from MEXT of Japan (Nos. 21108002, 24750054, 24750142, 25107510, 25246025, 25620037, 26708005, 26107510, 26110505, 26248017, 26620039, areas 2107 [Coordination Programming], 2406 [All Nippon Artificial Photosynthesis Project for

Living Earth], 2506 [Science of Atomic Layers], 2509 [Molecular Architectonics]). R.S. is grateful to The Tokuyama Science Foundation, Ogasawara Foundation for the Promotion of Science & Engineering, Japan Association for Chemical Innovation, The Kao Foundation for Arts and Sciences, The Asahi Glass Foundation, The Noguchi Institute, and The Iketani Science and Technology Foundation for financial support. T.K. appreciates the JSPS fellowship for young scientists. The theoretical work done at Univ. of Utah was supported by DOE-BES (Grant No.: DE-FG02-04ER46148). The authors acknowledge the Research Hub Advanced Nano Characterization (Graduate School of Engineering, The University of Tokyo) for the XPS and PES study.

■ REFERENCES

- (1) Novoselov, K. S.; Geim, A. K.; Morozov, S. V.; Jiang, D.; Zhang, Y.; Dubonos, S. V.; Grigorieva, I. V.; Firsov, A. A. *Science* **2004**, *306*, 666.
- (2) Novoselov, K. S.; Jiang, D.; Schedin, F.; Booth, T. J.; Khotkevich, V. V.; Morozov, S. V.; Geim, A. K. *Proc. Natl. Acad. Sci. U.S.A.* **2005**, *102*, 10451–10453.
- (3) Geim, A. K.; Novoselov, K. S. *Nat. Mater.* **2007**, *6*, 183–191.
- (4) Geim, A. K. *Science* **2009**, *324*, 1530–1534.
- (5) Lin, Y. M.; Dimitrakopoulos, C.; Jenkins, K. A.; Farmer, D. B.; Chiu, H.-Y.; Grill, A.; Avouris, Ph. *Science* **2010**, *327*, 662.
- (6) Mak, K. F.; Lee, C.; Hone, J.; Shan, J.; Heinz, T. F. *Phys. Rev. Lett.* **2010**, *105*, 136805.
- (7) Zande, A. M.; Huang, P. Y.; Chenet, D. A.; Berkelbach, T. C.; You, Y.-M.; Lee, G.-H.; Heinz, T. F.; Reichman, D. R.; Muller, D. A.; Hone, J. C. *Nat. Mater.* **2013**, *12*, 554–561.
- (8) Eda, G.; Yamaguchi, H.; Vohry, D.; Fujita, T.; Chen, M. *Nano Lett.* **2011**, *11*, 5111–5116.
- (9) Butler, S. Z.; Hollen, S. M.; Cao, L.; Cui, Y.; Gupta, J. A.; Gutierrez, H. R.; Heinz, T. F.; Hong, S. S.; Huang, J.; Ismach, A. F.; Johnston-Halperin, E.; Kuno, M.; Plashnitsa, V. V.; Robinson, R. D.; Ruoff, R. S.; Salahuddin, S.; Shan, J.; Shi, L.; Spencer, M. G.; Terrones, M.; Windl, W.; Goldberger, J. E. *ACS Nano* **2013**, *7*, 2898–2926.
- (10) Niyogi, S.; Bekyarova, E.; Hong, J.; Khizroev, S.; Berger, C.; Heer, W.; Haddon, R. C. *J. Phys. Chem. Lett.* **2011**, *2*, 2487–2498.
- (11) Yazyev, O. V.; Louie, S. G. *Nat. Mater.* **2010**, *9*, 806–809.
- (12) Bonaccorso, F.; Sun, Z.; Hasan, T.; Ferrari, A. C. *Nat. Photonics* **2010**, *4*, 611–622.
- (13) Bao, Q.; Loh, K. P. *ACS Nano* **2012**, *6*, 3677–3694.
- (14) Grigorenko, A. N.; Polini, M.; Novoselov, K. S. *Nat. Photonics* **2012**, *6*, 749–758.
- (15) Kambe, T.; Sakamoto, R.; Hoshiko, K.; Takada, K.; Miyachi, M.; Ryu, J.-H.; Sasaki, S.; Kim, J.; Nakazato, K.; Takata, M.; Nishihara, H. *J. Am. Chem. Soc.* **2013**, *135*, 2462–2465.
- (16) Hoshiko, K.; Kambe, T.; Sakamoto, R.; Takada, K.; Nishihara, H. *Chem. Lett.* **2014**, *43*, 252–253.
- (17) Murakami, S.; Nagaosa, N.; Zhang, S. C. *Phys. Rev. Lett.* **2004**, *93*, 156804.
- (18) Hasan, M. Z.; Kane, C. L. *Colloquium: topological insulators. Rev. Mod. Phys.* **2010**, *82*, 3045–3067.
- (19) Wang, Z. F.; Liu, Z.; Liu, F. *Phys. Rev. Lett.* **2013**, *110*, 196801.
- (20) Kong, D.; Cui, Y. *Nat. Chem.* **2011**, *3*, 845–849.
- (21) Moore, J. E.; Balents, L. *Phys. Rev. B* **2007**, *75*, 121306.
- (22) Hsieh, D.; Qian, D.; Wray, L.; Xia, Y.; Hor, Y. S.; Cava, R. J.; Hasan, M. Z. *Nature* **2008**, *452*, 970.
- (23) Fu, L.; Kane, C. L.; Mele, E. *Phys. Rev. Lett.* **2007**, *98*, 106803.
- (24) Xia, Y.; Qian, D.; Hsieh, D.; Wray, L.; Pal, A.; Lin, H.; Bansil, A.; Grauer, D.; Hor, Y. S.; Cava, R. J.; Hasan, M. Z. *Nat. Phys.* **2009**, *5*, 398–402.
- (25) Hong, S. S.; Kundhikanjana, W.; Cha, J. J.; Lai, K.; Kong, D.; Meister, S.; Kelly, M. A.; Shen, Z.-X.; Cui, Y. *Nano Lett.* **2010**, *10*, 3118–3122.

- (26) Hor, Y. S.; Richardella, A.; Roushan, P.; Xia, Y.; Checkelsky, J. G.; Yazdani, A.; Hasan, M. Z.; Ong, N. P.; Cava, R. J. *Phys. Rev. B* **2009**, *79*, 195208.
- (27) Cha, J. J.; Williams, J. R.; Kong, D.; Meister, S.; Peng, H.; Bestwick, A. J.; Gallagher, P.; Goldhaber-Gordon, D.; Cui, Y. *Nano Lett.* **2010**, *10*, 1076–1081.
- (28) Kong, D.; Dang, W.; Cha, J. J.; Li, H.; Meister, S.; Peng, H.; Liu, Z.; Cui, Y. *Nano Lett.* **2010**, *10*, 2245–2250.
- (29) Zhang, Y.; He, K.; Chang, C.-Z.; Song, C.-L.; Wang, L.-L.; Chen, X.; Jia, J.-F.; Fang, Z.; Dai, X.; Shan, W.-Y.; Shen, S.-Q.; Niu, Q.; Qi, X.-L.; Zhang, S.-C.; Ma, X.-C.; Xue, Q.-K. *Nat. Phys.* **2010**, *6*, 584.
- (30) Chen, Y. L.; Analytis, J. G.; Chu, J.-H.; Liu, Z. K.; Mo, S.-K.; Qi, X. L.; Zhang, H. J.; Lu, D. H.; Dai, X.; Fang, Z.; Zhang, S. C.; Fisher, I. R.; Hussain, Z.; Shen, Z.-X. *Science* **2009**, *325*, 178–181.
- (31) Bernevig, B. A.; Hughes, T. L.; Zhang, S. C. *Science* **2006**, *314*, 1757–1761.
- (32) König, M.; Wiedmann, S.; Brüne, C.; Roth, A.; Buhmann, H.; Molenkamp, L. W.; Qi, X.-L.; Zhang, S.-C. *Science* **2007**, *318*, 766–770.
- (33) Hirahara, T.; Bihlmayer, G.; Sakamoto, Y.; Yamada, M.; Miyazaki, H.; Kimura, S.-I.; Blügel, S.; Hasegawa, S. *Phys. Rev. Lett.* **2011**, *107*, 166801.
- (34) Yang, F.; Miao, L.; Wang, Z. F.; Yao, M.-Y.; Zhu, F.; Song, Y. R.; Wang, M.-X.; Xu, J.-P.; Fedorov, A. V.; Sun, Z.; Zhang, G. B.; Liu, C.; Liu, F.; Qian, D.; Gao, C. L.; Jia, J.-F. *Phys. Rev. Lett.* **2012**, *109*, 016801.
- (35) Wang, Z. F.; Liu, Z.; Liu, F. *Nat. Commun.* **2013**, *4*, 1471.
- (36) Wang, Z. F.; Su, N.; Liu, F. *Nano Lett.* **2013**, *13*, 2842–2845.
- (37) Sellmann, D.; Binder, H.; Häußinger, D.; Heinemann, F. W. *Inorg. Chim. Acta* **2000**, *300–302*, 829–836.
- (38) Zhou, S.; Ichimura, K.; Inokuchi, H. *J. Mater. Chem.* **1995**, *5*, 1725–1729.
- (39) Liu, S.-G.; Liu, Y.-Q.; Zhu, D.-B. *Synth. Met.* **1997**, *89*, 187–191.
- (40) Hobara, R.; Nagamura, N.; Hasegawa, S.; Matsuda, I.; Yamamoto, Y.; Miyatake, Y.; Nagamura, T. *Rev. Sci. Instrum.* **2007**, *78*, 053705.
- (41) Givaja, G.; Amo-Ochoa, P.; Garcia, C. J. G.; Zamora, F. *Chem. Soc. Rev.* **2012**, *41*, 115–147.
- (42) Low, K. H.; Roy, V. A. L.; Chui, S. S. Y.; Chan, S. L. F.; Che, C. M. *Chem. Commun.* **2010**, *46*, 7328–7330.
- (43) Coronado, E.; Mascaros, J. R. G.; Garcia, C. J. G.; Laukhin, V. *Nature* **2000**, *408*, 447.
- (44) Sun, D.; Luo, G.-G.; Zhang, N.; Xu, Q.-J.; Jin, Y.-C.; Wei, Z.-H.; Yang, C.-F.; Lin, L.-R.; Huang, R.-B.; Zheng, L.-S. *Inorg. Chem. Commun.* **2010**, *13*, 306–309.
- (45) Sheberla, D.; Sun, L.; Blood-Forsythe, M. A.; Er, S.; Wade, C. R.; Brozek, C. K.; Aspuru-Guzik, A.; Dincă, M. *J. Am. Chem. Soc.* **2014**, *136*, 8859–8862.

SUPPORTING INFORMATION

Redox Control and High Conductivity of Nickel Bis(dithiolene) Complex π -Nanosheet: A Potential Organic Two-Dimensional Topological Insulator

Tetsuya Kambe,[†] Ryota Sakamoto,[†] Tetsuro Kusamoto,[†] Tigmansu Pal,[†] Naoya Fukui,[‡] Ken Hoshiko,[†] Takahiro Shimojima,[§] Zhengfei Wang,[¶] Toru Hirahara,^{‡,‡} Kyoko Ishizaka,[§] Shuji Hasegawa,[‡] Feng Liu,[¶] and Hiroshi Nishihara^{†,*}

[†]Department of Chemistry, Graduate School of Science, The University of Tokyo, 7-3-1, Hongo, Bunkyo-ku, Tokyo 113-0033, Japan

[‡]Department of Physics, Graduate School of Science, The University of Tokyo, 7-3-1, Hongo, Bunkyo-ku, Tokyo 113-0033, Japan

[§]Quantum-Phase Electronics Center (QPEC) and Department of Applied Physics, Graduate School of Engineering, The University of Tokyo, 7-3-1, Hongo, Bunkyo-ku, Tokyo 113-8656, Japan

[¶]Department of Materials Science and Engineering, University of Utah, Salt Lake City, Utah 84112, United States

[‡]Current address: Department of Condensed Matter Physics, Graduate School of Science and Engineering, Tokyo Institute of Technology, 2-12-1, Ookayama, Meguro-ku, Tokyo 152-8551, Japan

*e-mail: nishihara@chem.s.u-tokyo.ac.jp

Methods

Materials. Ni(OAc)₂·4H₂O was purchased from Kanto Chemical Co., Inc. NaBr was received from Wako Pure Chemical Industries, Ltd. Tris(4-bromophenyl)aminium hexachloroantimonate was purchased from Sigma-Aldrich Co. Dichloromethane and ethyl acetate were distilled from NaH under a nitrogen atmosphere, and were stored with molecular sieves (4A, 1/16). Acetonitrile was purified with a Glass Contour Solvent Dispensing System (Nikko Hansen & Co., Ltd.). Water was purified using the Milli-Q purification system (Merck KGaA). Benzenehexathiol (BHT),¹ NaTCNQ,² and **ap-1**³ were synthesized according to the literatures.

Substrate pre-treatments. HOPG was purchased from Alliance Biosystems, Inc. (Grade SPI-1 10 × 10 × 2 mm), and cleaved with a piece of adhesive tape just before use. Silicon wafers (p-doped with a carrier concentration of 3 × 10¹⁸ cm⁻³) with thermally-grown 100-nm-thick SiO₂ were purchased from Yamanaka Semiconductor, and cut into squares (12 × 12 mm). An HMDS treatment for the silicon wafer was carried out in a petri dish: The cut silicon wafer was immersed in an ethanol solution (10 mL) of HMDS (100 μL) for 1 day. After annealing at 130°C for 2 min, the wafer was rinsed with ethanol and dried in vacuo.

Preparation of ox-1. Under an Ar atmosphere, **ap-1** (20.3 mg, equivalent to 13.8 μmol considering the nickel bis(dithiolene) complex unit) and tris(4-bromophenyl)aminium hexachloroantimonate (119 mg, 146 μmol) were added to dichloromethane (50 mL). The solution was stirred at room temperature for 22 h. Then the mixture was filtered through a membrane filter. The resultant black solid was washed with dichloromethane until the filtrate became colorless. After drying at 150 °C *in vacuo*, **ox-1** (black solid, 18.2 mg) was obtained.

Preparation of red-1. Under an Ar atmosphere, **ap-1** (10.0 mg, equivalent to 6.8 μmol considering the nickel bis(dithiolene) complex unit) and NaTCNQ (154 mg, 0.68 mmol) were added to acetonitrile (50 mL). The solution was refluxed for 15 h. Then the mixture was filtered through a membrane filter. The resultant black solid was washed with boiling acetonitrile until the filtrate became colorless. After drying at 150 °C *in vacuo*, **red-1** (black solid with metallic luster, 9.4 mg) was obtained.

XPS. The series of XPS was obtained using PHI 5000 VersaProbe (ULVAC-PHI, INC.). Al Kα (15 kV, 25 W) was used as the X-ray source, and the beam was focused on a 100 μm² area. The spectra were analyzed with MultiPak Software, and standardized using a C(1s) peak at 284.6 eV.

Electrical conductivity measurement. A home-made four-tip system⁴ was used for the conductivity measurement. Microflakes of **ap-1** and **ox-1** were deposited on the HMDS-modified silicon wafer using a dichloromethane and ethanol suspension. The four-tip made of tungsten was put on the microflake upon supervision of a scanning electron microscope (SEM, FEI™ Two lens electron column) furnished with the system. The authors also confirmed that the microflakes possessed flat and smooth textures using JEOL JSM-7400FNT SEM (Figure S4). The conductivity was measured by means of the van der Pauw method, from low temperatures to high temperatures. The thickness of the sample, 1 μm , was determined using AFM (Agilent Technologies 5500 equipped with a silicon cantilever PPP-NCL [Nano World], high-amplitude mode [trapping mode]). At each temperature, voltage-current (V - I) plots with one-thousand data points were acquired (Figure S5). The voltage spanned several mV, reversing the polarity (e.g. -5 mV \sim $+5$ mV). The resistance was extracted from the slope of the plot, which was then converted to the conductivity described in the main text.

Photoemission spectroscopy. Photoelectron emission spectroscopy was recorded using a hemispherical electron analyser (VG-SCIEN TA R4000). Single-layered **ap-1** was deposited 10 times onto the HOPG substrate, which was used as the sample. The sample was attached on the copper stage with Ag paste, and the surface of the stage was covered by carbon ink completely in order not to emit photoelectrons from metals. Photoemission spectra were recorded with He I radiation (21.2 eV) at a base vacuum of $< 5 \times 10^{-11}$ Torr. E_F was determined by the Fermi edge of an evaporated Au film connected to the sample electrically.

First principles calculation. First-principles band structure calculations of **ox-1** are carried out using VASP package⁵ with Perdew–Burke–Ernzerhof generalized gradient approximation. All of the calculations are performed with a plane-wave cutoff of 500 eV on $5 \times 5 \times 11$ Monkhorst-Pack k-point mesh. The lattice constants are chosen from the experimental data ($a = b = 14.1$ Å, $c = 7.6$ Å).³ During structural relaxation, all atoms are relaxed until the forces are smaller than 0.01 eV/Å.

S1–S3 Deconvolution of the S 2s peak in XPS.

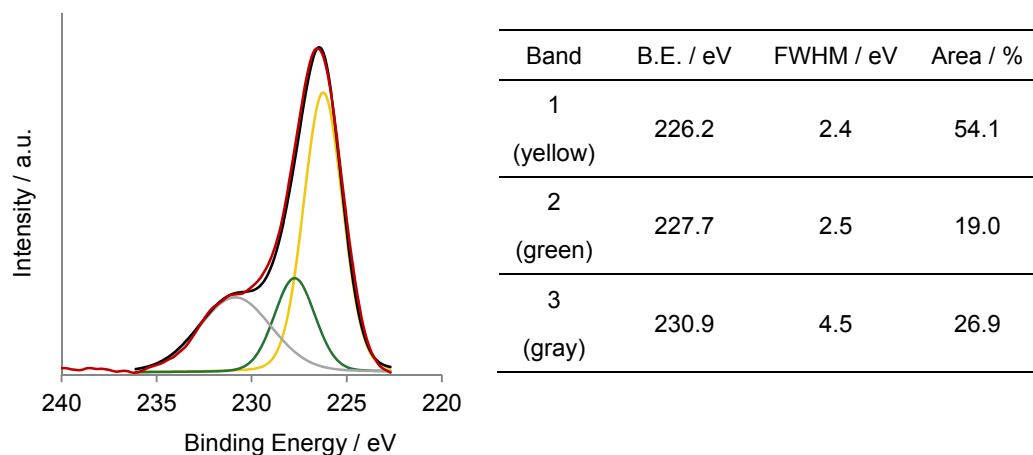


Figure S1. Deconvolution of the XPS S 2s peak of **ap-1**. The red line is the experimental spectrum. The yellow and green Gauss curves are derived from the nickel bis(dithiolene) moieties with -1 and 0 oxidation states, respectively. The gray one is assigned to the “shake-up” peak, which is often observed in bis(dithiolene) complexes.⁶ The black line is the sum of the Gauss curves. B.E. = binding energy.

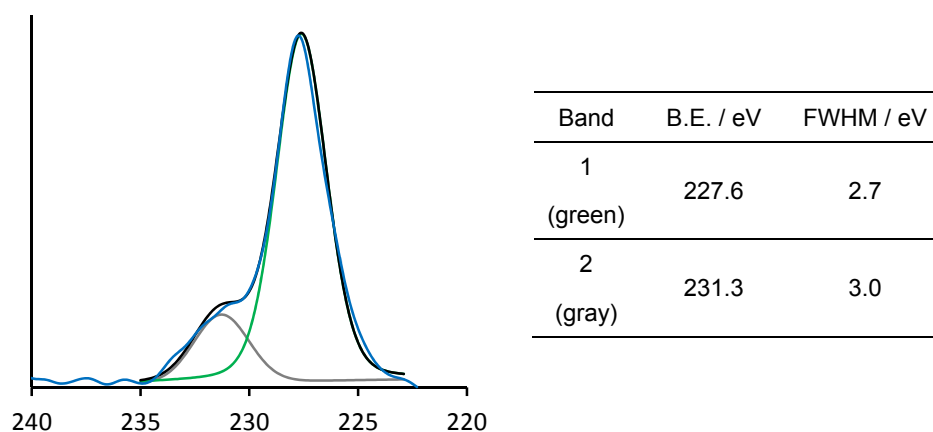


Figure S2. Deconvolution of the XPS S 2s peak of **ox-1**. The blue line is the experimental spectrum. The green Gauss curve is derived from the nickel bisdithiolene moiety in the 0 oxidation states. The gray one is assigned to the “shake-up” peak, which is often observed in bis(dithiolene) complexes.⁶ The black line is the sum of the Gauss curves. B.E. = binding energy.

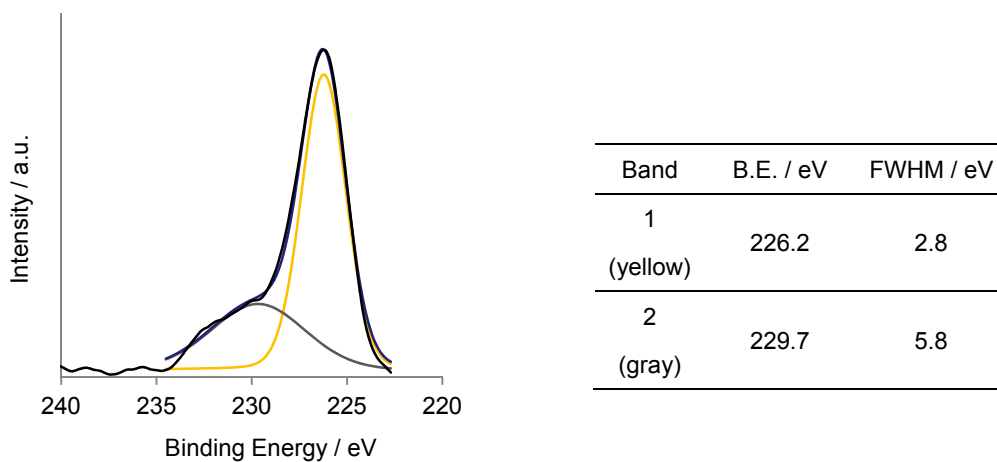


Figure S3. Deconvolution of the XPS S 2s peak of **red-1**. The black line is the experimental spectrum. The yellow Gauss curve is derived from the nickel bisdithiolene moiety in the -1 oxidation state. The gray one is assigned to the “shake-up” peak, which is often observed in bis(dithiolene) complexes.⁶ The dark-blue line is the sum of the Gauss curves. B.E. = binding energy.

S4 Close-ups of typical SEM images.

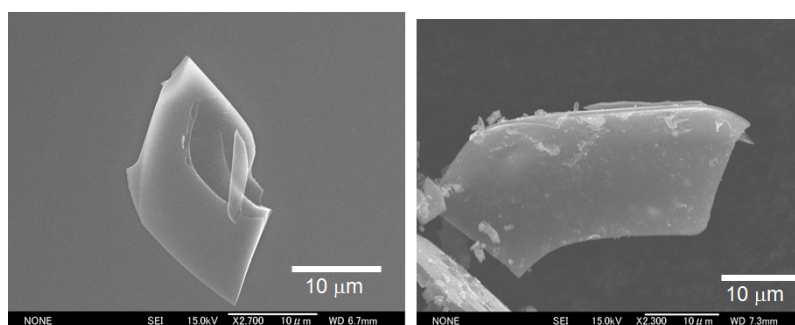


Figure S4. Close-ups of typical SEM images for **ox-1** (left) and **ap-1** (right) showing flat and smooth textures.

S5 Typical V - I plot.

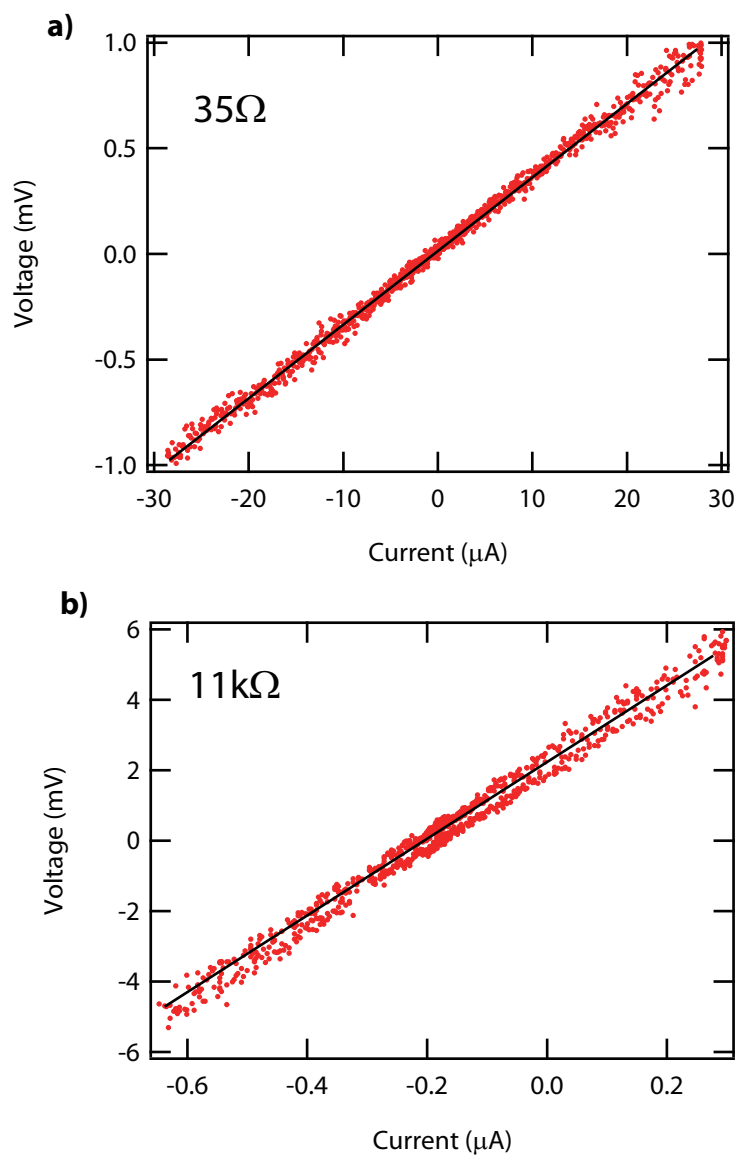


Figure S5. Typical V - I plot for (a) **ox-1** and (b) **ap-1**, respectively. The data points were acquired at 77 K. The linear fitting is based on the least squares method.

References for SI

1. Harnisch, J. A.; Angelici, R. J. *Inorg. Chim. Acta* **2000**, *300*, 273.
2. Melby, L. R.; Harder, R. J.; Hertler, W. R.; Mahler, W.; Benson, R. E.; Mochel, W. E. *J. Am. Chem. Soc.* **1962**, *84*, 3374.
3. Kambe, T; Sakamoto, R.; Hoshiko, K.; Takada, K.; Miyachi, M.; Ryu, J.-H.; Sasaki, S.; Kim, J.; Nakazato, K.; Takata, M.; Nishihara, H. *J. Am. Chem. Soc.* **2013**, *135*, 2462.
4. Hobara, R.; Nagamura, N.; Hasegawa S.; Matsuda, I.; Yamamoto, Y.; Miyatake, Y.; Nagamura, T. *Rev. Sci. Instrum.* **2007**, *78*, 053705.
5. Kresse, G.; Hafner, J. *Phys. Rev. B* **1993**, *47*, 558.
6. (a) Zhou, S.; Ichimura, K.; Inokuchi, H. *J. Mater. Chem.* **1995**, *5*, 1725. (b) Liu, S.-G.; Liu, Y.-Q.; Zhu, D.-B. *Synth. Met.* **1997**, *89*, 187.